Parameter Identification for the Preisach Model of Hysteresis

Daniel S. Joseph

Dissertation submitted to the Faculty of the
Virginia Polytechnic Institute and State University
in partial fulfillment of the requirements for the degree of

Doctor of Philosophy
in
Mathematics

Robert C. Rogers, Chair
Christopher Beattie
Jeff Borggaard
John Rossi
Robert Wheeler

April 24, 2001
Blacksburg, Virginia

Keywords: Least squares, Preisach measures, Scalar model

Parameter Identification for the Preisach Model of Hysteresis

Daniel S. Joseph

(ABSTRACT)

Hysteresis, defined as a rate independent memory effect, is a phenomenon that occurs in many physical systems. The effect is sometimes desired, it is sometimes a nuisance, it is sometimes catastrophic, but in every case we must understand hysteresis if we are to better understand the system itself. While the study of hysteresis has been conducted by engineers, scientists and mathematicians, the contribution of mathematicians has at times been theoretically sound but impractical to implement. The goal of this work is to use sound mathematical theory to provide practical information on the subject.

The Preisach operator was developed to model hysteresis in magnetism. It is based on a continuous linear combination of relay operators weighted by a distribution function μ. A new method for approximating μ in a finite dimensional space is described. Guidelines are given for choosing the "best" finite dimensional space and a "most efficient" training set. Simulated and experimental data are also introduced to demonstrate the utility of this method.

In addition, the approximation of singular Preisach measures is explored. The types of singularities investigated are characterized by non-zero initial slopes of reversal curves. The difficulties of finding the "optimal" approximation in this case are detailed as well as a method for determining an approximation "close" to the optimal approximation.

Acknowledgments

First and foremost, I thank my Lord, Jesus Christ, for giving me life and giving it abundantly. These four years have been a true blessing. "Every good and perfect gift is from above ..." James 1:17.

To my wife, Christine: You have been a part of everything I have accomplished since high school. You have worked much harder than I have these four years. Thank you for your undying support. You are my best friend. I love you.

To my children, Jacob, Micah, Rebecca, and Sarah: Thank you for helping me forget about work when I was home. You all bring such joy to my heart.

To my parents, Paul and Judy Joseph, and Christine's parents, Ron and Sally Roseveare: Thank you for your love and support. They are both so evident.

To Dr. Bob Rogers: Thank you for being such an excellent guide on this journey. You always seemed to be above it all looking at the big picture while I was beating at the weeds. I have learned a great deal from you. I look forward to working with you in the future.

To Eileen Shugart: Thank you for your patience and your example.

To Dr. Steve Galinaitis: Thank you for our discussions and for all of the time you spent on experimental data.

To Dr. Tao Lin: Thank you for the code to determine the projection on the continuous function space.

To my committee: Thank you for your time, especially Dr. Beattie whom I have bugged quite a few times with questions.

To my fellow grad students, past and present: There are several of you whom I should definitely mention by name, but I will refrain for fear of leaving someone out. To all of you with whom I have shared an office, classes, frustration, joy, a laugh, a computer question, and time on the basketball court.... Thanks.

Contents

List of Figures

List of Tables

Chapter 1

Background

1.1 Hysteresis in physical systems

Consider the following experiment. A torus of iron is annealed to bring it to a demagnetized state. A coil of wire is then wrapped around the iron ring and a current $\mathbf{I}$ is forced through the wire (see Figure 1.1). This current creates a magnetic field which we will call the applied magnetic field $\mathbf{H}$. The applied field $\mathbf{H}$ in turn induces a magnetism in the iron which yields a magnetic field that we will call $\mathbf{B}$. A second coil of wire is wrapped around the ring. The total flux Φ, created by the magnetic fields present in the system, is measured in this second coil. Because of the geometry of our described problem, the scalar input/output pair $(\mathbf{I}, \Phi)$ can reasonably be interpreted as representing the more complicated pair of vector fields $(\mathbf{H}, \mathbf{B})$.

We will refer to Figure 1.2 in order to investigate the relationship between $\mathbf{H}$ and the magnetization $\mathbf{M} := \mathbf{B} - \mathbf{H}$. As the current is increased $\mathbf{H}$ increases and the path traced out by the pair ($\mathbf{H}$, $\mathbf{M}$) follows 1. At a certain point the curve becomes almost horizontal. We call this "positive saturation" when further increase in the applied field yields little to no increase in the induced field. A subsequent decrease in the applied field causes ($\mathbf{H}$, $\mathbf{M}$) to trace path 2 (note here that $\mathbf{H}$ passing from positive to negative values indicates a reversal in the direction of current flow). Eventually, we reach the state of "negative saturation." Increasing $\mathbf{H}$ now causes the input/output pair to follow path 3. Continuing to alternate $\mathbf{H}$ between large positive and negative

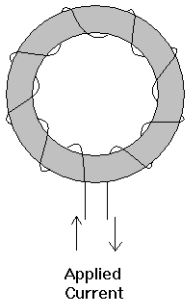

Figure 1.1: Iron torus experimental setup.

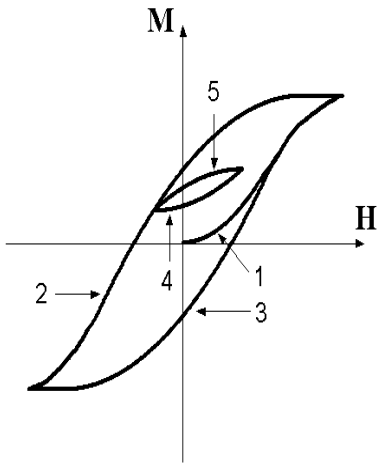

Figure 1.2: Simulated data from magnetic experiment.

values will essentially retrace paths 2 and 3. If we reverse the direction of $\dot{\mathbf{H}}$ at points other than negative or positive saturation ($\mathbf{H}$, $\mathbf{M}$) will trace out curves in the interior of path 2-3. An example of this is path $4-5$.

A quick review of Figure 1.2 reveals that $\mathbf{M}$ can not be written as a function of $\mathbf{H}$. Stated another way, $\mathbf{M}$ can not be determined simply by knowing the value of $\mathbf{H}$. The history of $\mathbf{H}$ must also be known to determine $\mathbf{M}$. This is because the output lags behind the input. Specifically, one can see that if we begin in the demagnetized state and increase $\mathbf{H}$ to the point of positive saturation, then remove the current, the iron ring will remain magnetized. (For more information on this experiment see for example [6]).

Now consider a different experiment. A piece of NiTi alloy wire is suspended vertically with a mass attached to its lower end. A current is applied to the wire which increases the temperature of the wire causing a change in its length. The change in length of the wire is measured by a sensor attached to the bottom. We then record a voltage, V_I, which is proportional to the input current and a voltage, V_O, from the displacement sensor.

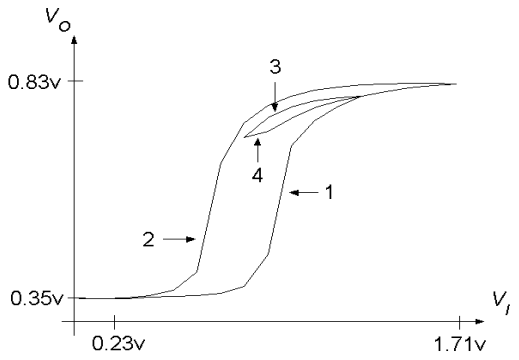

Figure 1.3: Simulated data from NiTi alloy wire experiment.

In Figure 1.3 we see that V_I can increase from $0v$ to $0.23v$ with no appreciable change in V_O. From $0.23v$ to $1.71v$ the input/output path traced by (V_I, V_O) follows 1. There is again no appreciable change in V_O when V_I is increased past $1.71v$ (once the wire reaches a certain temperature further increase in temperature will not change its length). The voltages $0.23v$ and $1.71v$ correspond to "negative" and "positive" saturation respectively. If we reach positive saturation and subsequently decrease V_I, (V_I, V_O) will follow path 2. Again, as in the magnetic experiment above, reversing the sign of $\dot{V}_I$ at a point other than negative or positive saturation will create interior curves (path 3-4).

1.2 Hysteresis defined

The type of input/output relationship seen in the experiments in Section 1.1 is called hysteresis and it occurs in many different areas. It can be found in the study of ferromagnetism, mechanical wear, phase transition, plasticity, smart materials and super-conductivity. This list is far from exhaustive. Recent

articles treating the effects of hysteresis can be found in journals of chemistry [1],[13], ecology [21], economics [8],[24], environmental studies [25], physics [18],[26], engineering [7],[19], and psychology [11]. What can we say about this relationship in an empirical sense?

Hysteresis is a multi-branching nonlinearity that occurs when the output of a system "lags behind" the input. This dissertation treats the case of *scalar hysteresis*, that is hysteresis occuring in a system with a scalar input and a scalar output. Mathematically, hysteresis is defined as a rate independent memory effect [14]. *Rate independence* implies that the path traced by the input/output pair (u, w) is invariant under any increasing time homeomorphism. In other words, if $u_1(t)$ and $u_2(t)$ are piecewise monotone functions on $(0, T]$ that have the same set of extrema which they reach in the same order, $\Gamma(u_1,\, w) = \Gamma(u_2,\, w)$ on $(0, T]$ even if u_1 and u_2 do not reach the extrema at the same rate. *Memory effect* implies that the output can not be determined simply by knowing the input, the history of the input must also be known. While not every physical system that displays hysteretic characteristics is strictly rate independent, this definition will satisfy the purposes of this paper.

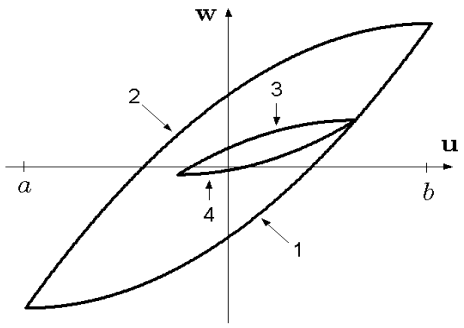

Figure 1.4: Signature hysteresis graph.

The "signature" hysteresis graph is shown in Figure 1.4. When the input reaches a we say that the system has reached *negative saturation*. This occurs when further decrease in the input yields little to no change in the output. Similarly we say that the system has reached *positive saturation* when the input increases to b. When the input increases from a to b, the pair (u, w) follows path 1, which is called the *limiting ascending branch* of the hysteresis loop because, in general, (u, w) will never be below this branch of the loop.

Similarly, 2 is called the *limiting descending branch.* Paths such as 3 and 4, called *reversal curves*, occur when the input reverses its direction at a point other than a or b.

1.3 Mathematical models of hysteresis

Because hysteresis occurs in so many different fields, the study of its effects has followed a variety of directions. Often models have been proposed for specific physical systems and later generalized to model hysteresis in other systems. Over the years there have been a number of mathematical models proposed, including the Duhem model, the Prandtl-Ishlinskii model, the Preisach model, the Stoner-Wohlfarth model, etc.. A description of these and additional models can be found in various monographs. (See, for example, monographs by Bertotti [4], Brokate and Sprekels [5], Della Torre [10], Mayergoyz [15] and Visintin [23].)

Two models that have received much attention in recent years have been the Preisach model [20] and the Stoner-Wohlfarth model [22]. The modeling of scalar hysteresis has been dominated by the Preisach model. It is a scalar model at its most basic level. Although the Stoner-Wohlfarth model has received much attention in vector hysteresis modeling, there have been recent attempts to extend the Preisach model to the vector case. Most notable are the continuous extension proposed by Mayergoyz [15] and the coupled-hysteron extension proposed by Della Torre [10]. Hybrid models combining the Preisach and Stoner-Wohlfarth models have also been introduced to model vector hysteresis [16].

This work concentrates on the scalar Preisach model. It is, however, quite reasonable to assume that the theory contained here could be extended to modifications of the Preisach model, including the previously mentioned vector models. It is the goal of the author to make these extensions at a later date.

Chapter 2

The Preisach Model

The Preisach model was originally introduced by Ferenc Preisach in 1935 [20] as a mathematical model for hysteresis in ferromagnetic materials. He created the model based on his understanding of the physics of magnetism: specifically, that materials are made up of tiny magnetic particles that he called hysterons which have a magnetic moment that depends on the history of an applied magnetic field. Since its introduction, however, many people have come to view the model in a phenomenological sense. Therefore, versions of the Preisach operator have been used as empirical models of hysteresis in a number of physical systems. Although the Preisach model was originated in the 1930's, rigorous mathematical treatment was not begun until the 1970's by a group of Russian mathematicians [14]. Since then there have been several monographs which have detailed treatments of the mathematical theory of the Preisach model. (See, for example, those by Bertotti [4], Brokate and Sprekels [5], and Visintin [23].) The objectives of this section are to

- Give a general description of the mathematical model.
- Describe some of the primary characteristics of the Preisach model.
- Describe several existing parameter identification methods.

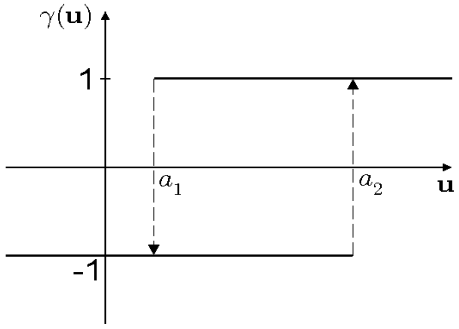

Figure 2.1: Delayed relay operator $\gamma_{(a_1,a_2)}$.

2.1 Description of the model

The building block of the Preisach model is a parameterized family of delayed relays $\gamma(u(t))$ (see Figure 2.1). Each relay in the family is characterized by its *switching values* $a_1 \leq a_2$. The output of the relay, which can take on the values ± 1, remains constant until the input increases above a_2 (at which point the output jumps to 1) or decreases below a_1 (at which point it jumps to -1). These jumps are "irreversible" if $a_1 \neq a_2$. We choose the convention of parameterizing a relay by the average of its switching values $s = \frac{a_1+a_2}{2}$ and the half-width of its switching values $r = \frac{a_2-a_1}{2}$. We can represent the relay in the following manner. Given an input function $u(t) \in C([0,T])$

$$\gamma_{(r,s)}(u(t)) = \begin{cases} -1 & u(t) < s - r, \\ \gamma_{(r,s)}(u(t^-)) & s - r \leq u(t) \leq s + r, \\ 1 & u(t) > s + r. \end{cases} \tag{2.1}$$

Here $u(t^-) = \lim_{z \to t^-} u(z)$, and we assume $\gamma_{(r,s)}(u(0^-)) := \gamma_0 \in \{-1, 1\}$, the initial state of the relay, is prescribed. We can see that when $a_1 \leq u(t) \leq a_2$ the output can not be determined simply by knowing the input. The history of the input must also be known. (Note that traditionally when $\gamma(u(t)) = 1$ we say that the relay is in the "on" position and when $\gamma(u(t)) = -1$ we say that the relay is in the "off" position).

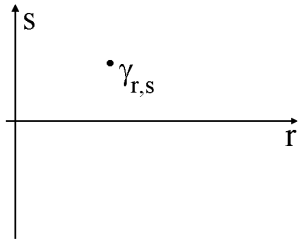

Figure 2.2: The Preisach plane.

2.1.1 The geometry of the Preisach plane

We now define the *Preisach plane* $\mathcal{P} := \{(r,s) \in \mathbb{R}^2 \mid r \geq 0\}$. Each point $\rho = (r,s)$ in the Preisach plane represents a relay, γ_ρ (see Figure 2.2). We will assume that the initial state of the Preisach plane, that is the state of all relays γ_ρ prior to applying the input $u(t)$, is the *virgin state*. In the virgin state $\gamma_{(r,s)} = -1$ for $s > 0$ and $\gamma_{(r,s)} = +1$ for $s < 0$. While this assumption may seem artificial, we will see later that for our purposes it causes no loss of generality.

With the application of the input $u(t) \in C([0,T])$, various relays in the plane switch. The action of the relays defines a "Preisach state function"

$$\mathcal{P} \ni \rho \mapsto \xi_{u(t)}(\rho) := \gamma_\rho(u(t)) \in \{-1, 1\} \tag{2.2}$$

and creates the following sets:

$$\begin{aligned} A_+(t) &:= \text{interior}(\{\rho \in \mathcal{P} \mid \xi(\rho) = \gamma_\rho(u(t)) = 1\}) \\ A_-(t) &:= \text{interior}(\{\rho \in \mathcal{P} \mid \xi(\rho) = \gamma_\rho(u(t)) = -1\}) \\ B_\xi(t) &:= \{\rho \in \mathcal{P} \mid \rho \in \partial A_+(t) \cap \partial A_-(t)\} \end{aligned}$$

The set $B_\xi(t)$ is called the *dividing line* at time t. As $u(t)$ is applied one can see that $s > u(t) + r$ implies that $\rho = (r,s) \in A_-(t)$ and $s < u(t) - r$ implies that $\rho = (r,s) \in A_+(t)$ (see Figure 2.3). As $u(t)$ decreases it "sweeps" all ρ above the line $s = u(t) + r$ into $A_-(t)$. Similarly, as $u(t)$ increases it "sweeps" all ρ below $s = u(t) - r$ into $A_+(t)$. This sweeping action gives rise to dividing lines $B_\xi(t)$ which are graphs of *memory curves*

$$M := \{\phi \in C_c(\mathbb{R}_+) \mid |\phi'(r)| = 1 \text{ for almost all } r \in \text{ support}(\phi)\}$$

Figure 2.4 shows the graph of a memory curve $\phi_{u(t)}$ parameterized by the input $u(t)$ which begins at $u(0) = 0$ and has relative extrema (ordered by time) given by

$$0, u_1, u_2, u_3 = u(T_1)$$

We note here that given $T_2 > T_1$ and the new set of time ordered extrema

$$0, u_1, u_2, u_3, u_4 = u(T_2)$$

all effects of the extrema u_2 and u_3 are removed (see Figure 2.5). This phenomenon, a general property of the Preisach operator called the *wiping out principle*, is described in the following paragraph.

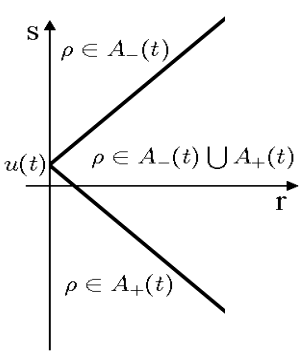

Figure 2.3: Application of $u(t)$ to the Preisach plane.

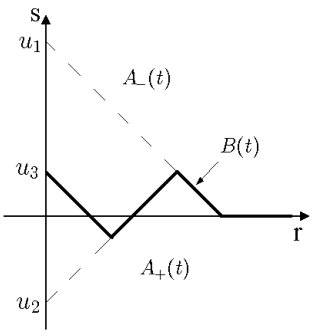

Figure 2.4: Memory curve $\phi_{u(T_1)} = u_3$.

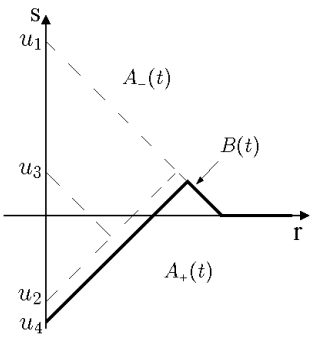

Figure 2.5: Memory curve $\phi_{u(T_2)} = u_4$.

We will define an *alternating series of dominant input extrema* to be a time ordered list of maximums (M_i) and minimums (m_i) of the function $u(t) \in C([0,T])$ on $[0,t_1]$

$$M_1, m_1, M_2, m_2, \cdots, M_n, m_n, M_{n+1}, m_{n+1}, \cdots, M_k, m_k \tag{2.3}$$

such that $M_1 > M_2 > \cdots > M_k$, and $m_1 < m_2 < \cdots < m_k$. (The list can begin or end with either a maximum or a minimum, for the sake of brevity we will only consider the above case.) If we observe u on (t_1, t_2) and a new maximum M_{k+1} occurs such that $M_n > M_{k+1} > M_{n+1}$ then the new alternating series of dominant input extrema will be

$$M_1, m_1, M_2, m_2, \cdots, M_n, m_n, M_{k+1} \tag{2.4}$$

The extrema $M_{n+1}, m_{n+1}, \cdots, M_k, m_k$ at the end of (2.3) do not exist in (2.4). They have been "wiped out." Mayergoyz has proven the following theorem [15, p.15].

Theorem 2.1.1 (The Wiping-Out Property). *Only the alternating series of dominant input extrema are stored by the Preisach model. All other input extrema are wiped out.*

2.1.2 The Preisach operator

We now define the Preisach operator to be

$$[\mathcal{H}_\mu(u, \xi_\rho)](t) := \int_{\mathcal{P}} [\gamma_\rho(u, \xi_\rho)](t) d\mu(\rho) \qquad \forall t \in [0,T] \tag{2.5}$$

where

- μ is a finite signed Borel measure over $\mathcal{P}$,
- $u \in C([0,T])$,
- ξ_ρ is a Preisach state function (see (2.2)) describing the initial state of the Preisach plane, and
- $\gamma_\rho(u,\xi_\rho) := \gamma_\rho(u)$ with the initial state given by ξ_ρ.

In essence, the Preisach operator is an infinite linear combination of simple relays weighted by the measure μ. We can classify the operator as a map

$$\mathcal{H}_\mu : C([0,T]) \times \text{“Preisach state functions”} \to L^\infty \bigcap C_r^0([0,T)) \tag{2.6}$$

Although (2.6) allows for discontinuous Preisach operators, we are only concerned with continuous Preisach operators. For this reason we impose the restriction

$$|\mu|\{\bigcup_{r\in\mathbb{R}_+}(r,c+r)\} = |\mu|\{\bigcup_{r\in\mathbb{R}_+}(r,c-r)\} = 0 \qquad \forall c \in \mathbb{R} \tag{2.7}$$

Visintin [23, p.112] has shown the following.

Theorem 2.1.2 (Conditions for $\mathcal{H}_\mu(\cdot,\xi) \in C^0([0,T])$). *Let μ be a finite signed Borel measure over $\mathcal{P}$ and ξ a Preisach state function. Then*

$$\mathcal{H}_\mu(\cdot,\xi) : C^0([0,T]) \to C^0([0,T])$$

if and only if μ satisfies (2.7).

It is somewhat standard practice at this point to restrict the support of μ to a limiting triangle $\mathcal{T}$ (Figure 2.6). This is reasonable, not only with regard to the mathematical model (since μ is a finite measure, for any $\epsilon > 0$ we can choose $\mathcal{T}$ such that $|\mu|\{\mathcal{P}\backslash\mathcal{T}\} < \epsilon$), but also with regard to the physical systems in question (the occurance of negative and positive saturation).

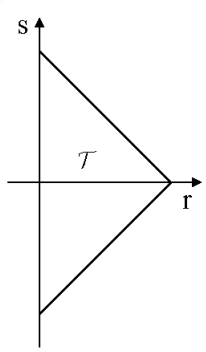

Figure 2.6: The limiting triangle $\mathcal{T}$.

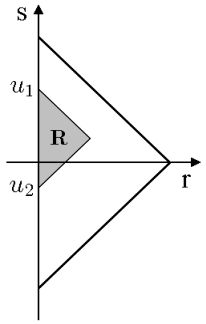

Figure 2.7: When u cycles between u_1 and u_2, the region $\mathbf{R}$ is swept out.

Now the Preisach operator becomes

$$[\mathcal{H}_\mu(u,\xi)](t) = \int_{\mathcal{T}} [\gamma_\rho(u,\xi_\rho)](t) d\mu(\rho) \qquad \forall t \in [0,T] \tag{2.8}$$

If we begin at time t_0 with the input at negative saturation we will have $\rho \in A_-(t_0) \quad \forall \rho \in \mathcal{T}$. (This is why we lost no generality by assuming that the initial state was the virgin state earlier. All relays will be taken to the off position with the application of $u(t_0)$.) Monitoring the state of the limiting triangle is now a simple matter of recording the dominant series of input extrema.

Before moving on we will describe one other general property of the Preisach operator called the *Congruency property.* We can see in Figure 2.7 that if we cycle the input between the extrema u_1 and u_2 the Preisach state

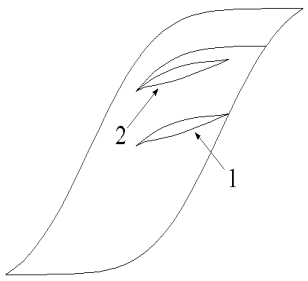

Figure 2.8: Congruent loops of a Preisach operator.

function will continue to sweep out the same region, **R**. Regardless what the prior history of the input is, the loops in the input/output graph created by this cyclic input will be congruent. In other words, the loops will have the same shape. The only difference will be a possible displacement in the s direction. This is illustrated by the loops labeled 1 and 2 in Figure 2.8. This property is stated in the following theorem introduced by Mayergoyz [15, p.17].

Theorem 2.1.3 (Congruency Property). *All minor hysteresis loops corresponding to input cycles between two consecutive input extrema are congruent.*

In an effort to characterize the Preisach operator, Mayergoyz has proven that Theorem 2.1.1 and Theorem 2.1.3 are the necessary and sufficient conditions for representing hysteretic effects by the Preisach model [15, p.24].

Theorem 2.1.4. *The wiping-out property and the congruency property constitute the necessary and sufficient conditions for a hysteresis nonlinearity to be represented by the Preisach model on the set of piecewise monotonic inputs.*

2.2 Parameter identification

The issue of parameter identification is naturally important in any empirical model, but is particularly so in a model applied to a wide variety of physical systems. We can see from the previous discussion that determining the output of the Preisach operator is a matter of

- knowing the state of the Preisach plane and
- knowing the parameter μ in the Preisach operator.

In order to use the Preisach operator to model a system with hysteresis we must identify an "optimal" parameter μ corresponding to data obtained from that system. In this section we will discuss several existing methods for determining that optimal parameter.

2.2.1 Standard experimental measurements

In ferromagnetism, the parameter μ is seen as a probability distribution of hysterons. This led Della Torre and his co-authors to assume a particular form for μ, namely the Gaussian function

$$\mu(r,s) = \frac{M_{\text{sat}}}{2\pi\sigma_i\sigma_k} \exp\{-\frac{1}{2}[\frac{(r-h_k)^2}{\sigma_k^2} + \frac{s^2}{\sigma_i^2}]\} \tag{2.9}$$

The beauty of this method is in its simplicity. The measure μ has four unknown parameters $(M_{\text{sat}}, h_k, \sigma_k, \sigma_i)$ which can easily be determined with only a few measurements, and these are standard in experimental magnetism. In fact, only measurements on the limiting branches and one reversal curve are required. Once these parameters are determined the measure μ is known over the entire Preisach plane. The obvious limitation with this method, however, is that we have been quite restrictive on μ, requiring it to be Gaussian in form. This inhibits the curve fitting method from being applied to a wide variety of physical systems.

2.2.2 Interpolation

A second method for approximating the parameter is to determine the value of the parameter at various points in the limiting triangle and use interpolation to approximate μ over the remainder of the limiting triangle. Unfortunately, to determine the value of μ at these points one must take second differences of experimentally determined quantities. This can greatly magnify any error introduced in the collection of data.

Mayergoyz has modified this method to remove the difficulty of taking second difference quotients. (See [15] for a detailed treatment.) He sets as his goal not determining the parameter μ, but determining a function f which describes the effect of μ on the hysteresis operator. This function is determined at various points throughout the limiting triangle and then interpolated.

The methods described in this section allow for a much more general parameter and therefore are applicable in a greater number of physical systems. They do, however, require the collection of much more data than the curve fitting method described above.

2.2.3 Other methods

Other methods exist for the determination of the parameter μ in the Preisach operator. Some (e.g. Banks, Kurdila, and Webb [2]) even modify the Preisach operator in order to allow for more general measures. The goal of this work is to allow for a somewhat general parameter while maintaining the Preisach operator. We want to set forth a method of identification which is accurate, easy to implement, and allows for approximation in an adaptive setting.

Chapter 3

Least Squares Parameter Identification

In this section we introduce a new method for parameter identification in the Preisach model. We attempt to take advantage of the duality relationship between the state of the Preisach plane and the parameter μ. A least squares scheme is used to approximate the measure in a rather general setting. Least squares has the advantages of providing a rational way of dealing with incomplete data and allowing for adaptive identification of parameters. The key to this method is choosing the correct approximation space.

3.1 Theoretical background

We begin the discussion by revisiting the Preisach operator. In order to allow for a relatively general class of measures while taking advantage of the inherent duality in the operator, we define the space of *Preisach measures*

$$\mathcal{M} := \{\text{finite Borel measures } \mu \text{ on } \mathcal{P} \mid \mu \in L^2(\mathcal{P}), \text{support}(\mu) \subset \mathcal{T}\}$$

This is far from the most general class possible (as Theorem 2.1.2 indicates) but has been a common assumption in applications. Of course, we can now place the usual $L^2(\mathcal{T})$ Hilbert space structure on the Preisach measures. We

use the inner product

$$\langle \mu, \nu \rangle := \langle \mu, \nu \rangle_{L^2(\mathcal{T})} = \int_{\mathcal{T}} \mu\nu \; ds \; dr,$$

and we define the usual norm $\|\mu\| := \sqrt{\langle \mu, \mu \rangle}$ on $\mathcal{M}$. We also define the class of *Preisach state functions*

$$\mathcal{S} := \{\xi : \mathcal{P} \to \{1, -1\} \mid B_\xi = \text{ graph}(\phi) \text{ for some } \phi \in M\}.$$

Note that if we restrict the state functions to $\mathcal{T}$ then, $\mathcal{S} \subset \mathcal{M}$.

Now, for a given $\mu \in \mathcal{M}$ we define the Preisach operator $\mathcal{H}_\mu : C[0,T] \to \mathbb{R}$ by

$$\mathcal{H}_\mu(u(t)) = \int_{\mathcal{T}} \xi_{u(t)} d\mu = \langle \xi_{u(t)}, \mu \rangle.$$

We can think of the Preisach operator as the composition of the (highly) nonlinear *state operator*

$$C[0,t] \ni u(\cdot) \mapsto \xi_{u(t)} \in \mathcal{S}$$

with the linear inner product pairing between the state functions and a fixed Preisach measure

$$\mathcal{S} \ni \xi_{u(t)} \mapsto \langle \xi_{u(t)}, \mu \rangle \in \mathbb{R}.$$

We think of the inner product action

$$\langle \xi, \mu \rangle$$

as an *observation* of the measure $\mu \in \mathcal{M}$ under the state $\xi \in \mathcal{S}$.

We now consider the problem of identifying an "optimal" Preisach measure corresponding to data obtained from a system with hysteresis. Suppose $\{d_i\}_{i=1}^M$ is a set of scalar output data corresponding to a sequence of Preisach state functions $\{\xi_i\}_{i=1}^M$. (The state functions could correspond to the states generated by "training data" defined by the history of a particular input function $u \in C[0,T]$ at times $\{t_i\}_{i=1}^M$, but this is not necessary.) We seek an optimal measure in $\mathcal{M}_N$, an N dimensional subspace of $\mathcal{M}$.

Problem 3.1.1 (Identification from data). Suppose $\mathcal{M}_N$ is an N dimensional subspace of $\mathcal{M}$. Given a set of data $\{d_i\}_{i=1}^M$ and the corresponding Preisach state functions $\{\xi_i\}_{i=1}^M$ find $\bar{\mu} \in \mathcal{M}_N$ such that

$$\sum_{i=1}^{M} |\langle \xi_i, \bar{\mu} \rangle - d_i|^2 = \min_{\tilde{\mu} \in \mathcal{M}_N} \quad \sum_{i=1}^{M} |\langle \xi_i, \tilde{\mu} \rangle - d_i|^2. \tag{3.1}$$

This is a standard linear least squares problem. To put it in a more familiar form let $\{\mu_i\}_{i=1}^N$ be an orthonormal basis for $\mathcal{M}_N$ and let

$$A = \begin{bmatrix} a_{1,1} & a_{1,2} & \cdots & a_{1,N} \\ a_{2,1} & a_{2,2} & \cdots & a_{2,N} \\ \vdots & & \ddots & \vdots \\ a_{M,1} & a_{M,2} & \cdots & a_{M,N} \end{bmatrix}. \tag{3.2}$$

where $a_{i,j} = \langle \xi_i, \mu_j \rangle$. Let $\mathbf{d} := (d_1, d_2, \ldots, d_M)^T \in \mathbb{R}^M$ be the vector of data points. Then simply taking inner products above shows that the problem of finding a solution $\bar{\mu} = \sum_{i=1}^N \bar{x}_i \mu_i \in \mathcal{M}_N$ of the identification Problem 3.1.1 is equivalent to finding $\bar{\mathbf{x}} \in \mathbb{R}^N$ such that

$$|A\bar{\mathbf{x}} - \mathbf{d}|^2 \leq |A\mathbf{x} - \mathbf{d}|^2 \ \ \forall \mathbf{x} \in \mathbb{R}^N.$$

Here $|\cdot|$ is the Euclidean norm on $\mathbb{R}^N$. Standard results (cf. e.g. [3]) on this problem include the following.

- If either $M < N$ (fewer observations than unknowns) or A has less than full rank, there is an infinite family of solutions. There is a unique solution with minimal Euclidean norm.
- If $M > N = \text{rank}(A)$ then there is a unique solution to the least squares problem, but generically the data is not fit exactly, i.e. $A\bar{\mathbf{x}} \neq \mathbf{d}$.
- If $M = N = \text{rank}(A)$ then there is a unique solution that does fit the data exactly.

We identify sufficient conditions to ensure that the matrix A has full rank below. However, before examining these conditions, let us consider the special case where the identification problem is applied to data coming from observations of a given Preisach measure.

Problem 3.1.2 (Identification from a given measure). Suppose $\mu \in \mathcal{M}$ is given and $\mathcal{M}_N$ is an N dimensional subspace of $\mathcal{M}$. Given a set of Preisach state functions $\{\xi_i\}_{i=1}^M$ and corresponding observations of the measure μ, $d_i = \langle \xi_i, \mu \rangle$, find $\bar{\mu} \in \mathcal{M}_N$ such that

$$\sum_{i=1}^M |\langle \xi_i, \bar{\mu} \rangle - d_i|^2 = \min_{\widetilde{\mu} \in \mathcal{M}_N} \quad \sum_{i=1}^M |\langle \xi_i, \widetilde{\mu} \rangle - d_i|^2 = \min_{\widetilde{\mu} \in \mathcal{M}_N} \quad \sum_{i=1}^M |\langle \xi_i, \widetilde{\mu} - \mu \rangle|^2 \tag{3.3}$$

In a sense, this identification problem is one of approximating μ by $\bar{\mu}$. Of course, in a Hilbert space setting, there is another "approximation problem" for the measure μ.

Problem 3.1.3 (Best approximation to a given measure). Given $\mu \in \mathcal{M}$ and an N-dimensional subspace $\mathcal{M}_N \subset \mathcal{M}$, find $\hat{\mu} \in \mathcal{M}_N$ that provides the "best approximation" to μ in $\mathcal{M}_N$, i.e.

$$\|\hat{\mu} - \mu\| = \min_{\widetilde{\mu} \in \mathcal{M}_N} \|\widetilde{\mu} - \mu\| \tag{3.4}$$

The projection theorem guarantees a unique solution to this problem. To compute it, let $\{\mu_i\}_{i=1}^N$ be an orthonormal basis for $\mathcal{M}_N$. Then we can write

$$\mu = \hat{\mu} + \nu = \sum_{j=1}^{N} \langle \mu, \mu_j \rangle \mu_j + \nu = \sum_{j=1}^{N} \beta_j \mu_j + \nu,$$

where $\nu \in \mathcal{M}_N^{\perp}$. The measure $\hat{\mu}$ is the projection of μ onto $\mathcal{M}_N$.

Are the two problems above the same? Surprisingly enough, the answer is "generally not." This is true even when the least squares problem has a unique solution that fits the data exactly.

To see this, note that each $\xi_i \in \mathcal{S}$ can be written as $\xi_i = \sum_{j=1}^{N} a_{i,j}\mu_j + l_i$ where $a_{i,j} = \langle \xi_i, \mu_j \rangle$ are the components of A given above and $l_i \in \mathcal{M}_N^{\perp}$. Thus, for any $\widetilde{\mu} = \sum_{i=1}^{N} \alpha_i \mu_i \in \mathcal{M}_N$ we have

$$\begin{aligned}
\sum_{i=1}^{M} |\langle \xi_i, \widetilde{\mu} - \mu \rangle|^2 &= \sum_{i=1}^{M} |\langle \sum_{j=1}^{N} a_{i,j}\mu_j + l_i, \sum_{k=1}^{N} (\alpha_k - \beta_k)\mu_k - \nu \rangle|^2 \\
&= \sum_{i=1}^{M} |\sum_{j=1}^{N} a_{i,j} \sum_{k=1}^{N} (\alpha_k - \beta_k)\langle \mu_j, \mu_k \rangle - \langle l_i, \nu \rangle|^2 \\
&= \sum_{i=1}^{M} |\sum_{j=1}^{N} a_{i,j}(\alpha_j - \beta_j) - \langle l_i, \nu \rangle|^2
\end{aligned}$$

The identification problem is equivalent to minimizing the last quantity over $\alpha \in \mathbb{R}^n$. Note that unless we have $\langle l_i, \nu \rangle = 0$ for all i, we can not ensure that this is minimized at $\alpha_j = \beta_j$. Thus, the measure given by the identification is generally *not* the projection. We summarize this in the following.

Theorem 3.1.1. *Unless $\xi_i \in \mathcal{M}_N$ for $i = 1, \ldots, M$, identifying a general measure μ from these state functions does not in general yield the best approximation to μ. In particular, if $\mathcal{M}_N$ is a space of continuous functions, then no sequence of state observations can always identify the best approximation of μ. On the other hand, if $\xi_i \in \mathcal{M}_N$ for all i and the matrix A given by (3.2) is full rank, the identification problem for any measure does yield the best approximation to that measure.*

With this theorem in mind, let us define $\mathcal{M}_N$ for which we can choose state functions $\{\xi_i\}_{i=1}^M \subset \mathcal{M}_N$ such that A is full rank. We do this by discretizing the limiting triangle $\mathcal{T}$ using a rotated square mesh with $n+1$ nodes along the s-axis. This discretization can be used to divide $\mathcal{T}$ into $N = \frac{n^2+n}{2}$ regions as shown in Figure 3.1. We now define

$$\mathcal{M}_N := \{\mu \in L^2(\mathcal{T}) \mid \mu = \sum_{i=1}^{N} \alpha_i \mu_i\}$$

where $\alpha_i \in \mathbb{R}$ and μ_1, μ_2, $\cdots$, μ_N are the characteristic functions of the triangular and diamond shaped regions in Figure 3.1.

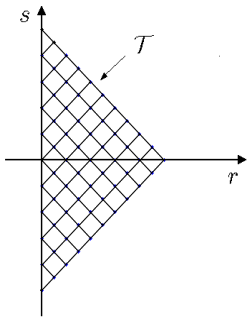

Figure 3.1: Rotated square mesh discretization of $\mathcal{T}$.

With a simple algorithm we determine a "most efficient" set of training data that will ensure a square matrix A of full rank.

- We begin with the initial state of negative saturation. We then record state functions and data from first reversal curves with incrementally higher input extrema.
- These input extrema, and the data collection points on the reversal curves, correspond to the boundaries between the n triangular regions along the s-axis in our discretization.

Chosen this way the discontinuities in the state functions occur only along the boundaries of the regions. Thus the state functions are all in the span of the basis vectors for $\mathcal{M}_N$. Figures 3.2, 3.3, and 3.4 refer to the above algorithm.

If we do not record data at negative saturation (this is not necessary since we record data at positive saturation and the two states will give us the same information about the limiting triangle) then the algorithm yields N data points and state functions. In addition, the matrix A determined by the state functions is full rank. We call this a most efficient set of training data because N is the minimum number of state functions that will yield a full rank matrix A since $\mathcal{M}_N$ is N dimensional.

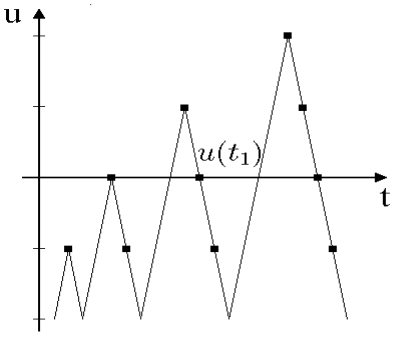

Figure 3.2: Sample input with data collection points for "most efficient" training set.

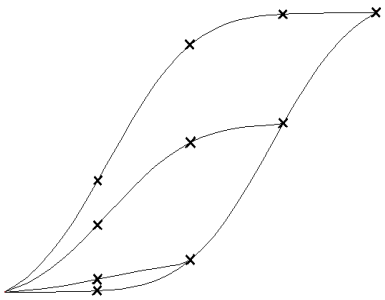

Figure 3.3: Hysteresis loop with data collection points.

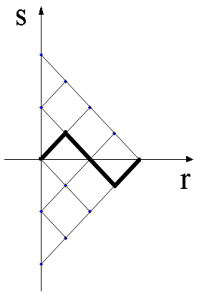

Figure 3.4: Graph of the memory curve $\phi_{u(t_1)}$ corresponding to $\xi_{u(t_1)}$.

There is a major concern that emerges when implementing a method like the one described above: how sensitive is the approximation method to experimental errors in the input? In the method that we are introducing, a strong indicator of the sensitivity is the condition number of the matrix A. (Note that the matrix A that is discussed here and used in the calculations is a scaled version of the one whose entries are $a_{i,j} = \langle \xi_i, \mu_j \rangle$). If A has a large condition number it is possible for the model to be very sensitive to errors in the input, while a low condition number for A would imply that the model is quite stable and would not be greatly effected by small errors in the input.

The high degree of structure in the matrix A allows us to characterize the condition number of A. Table 3.1 shows the condition numbers of the matrices determined by the algorithm described in this section for several different finite dimensional spaces $\mathcal{M}_{10}, \mathcal{M}_{36}, \mathcal{M}_{136}, \mathcal{M}_{528}$ and $\mathcal{M}_{2080}$. (Note

Subspace	triangles along s-axis	Size of A	cond(A)	$\|A\|_\infty$	$\|A^{-1}\|_\infty$
$\mathcal{M}_{10}$	4	10×10	16	8	2
$\mathcal{M}_{36}$	8	36×36	64	32	2
$\mathcal{M}_{136}$	16	136×136	256	128	2
$\mathcal{M}_{528}$	32	528×528	1024	512	2
$\mathcal{M}_{2080}$	64	2080×2080	4096	2048	2

Table 3.1: Condition number of the matrix A for various spaces $\mathcal{M}_N$.

as before for $\mathcal{M}_N, N = \frac{n^2+n}{2}$ where n is the number of triangles along the s-axis in the discretization). Because $|a_{i,j}| = \frac{1}{2}$ for $1 \leq i \leq n$ and $|a_{i,j}| = 1$ for $n+1 \leq i \leq \frac{n^2+n}{2}$ we have $\|A\|_\infty = \frac{n^2}{2}$. It is more difficult to show, however, that $\|A^{-1}\|_\infty = 2$. This work is in progress, but to date we must limit the following result to a conjecture.

Conjecture 3.1.2. *Given the $N \times N$ matrix A determined by the method described above where $N = \frac{n^2+n}{2}$ (n is the number of triangles along the s-axis in the discretization of $\mathcal{T}$), then cond$(A) = n^2$. Here cond(A) is the condition number of A induced by the infinity norm. This implies that the condition number of A grows linearly with the size of A.*

3.2 Approximations using simulated data

We have stated theoretical results that suggest the benefits of approximating the Preisach measure by a step function. In this section we employ simulated data to illustrate these benefits by contrasting the measures found by projection and identification for different finite dimensional spaces. For our simulation we use a form of the Preisach measure given by Della Torre [10, p. 41]. (See Figure 3.5).

$$\mu(r,s) = \frac{2}{\pi}\exp[-2((r-3)^2 + s^2)]$$

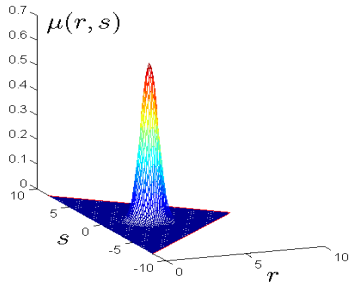

Figure 3.5: Graph of $\mu(r, s)$.

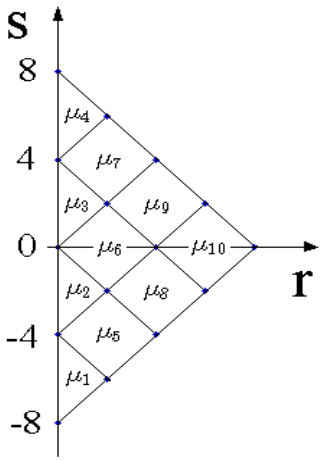

Figure 3.6: Regions of $\mathcal{T}$ in $\mathcal{M}_{10}$.

First, we approximate the Preisach measure μ in a space of step functions. Assume a limiting triangle, $\mathcal{T}$, with endpoints $(0, -8)$, $(0, 8)$ and $(8, 0)$. Now discretize $\mathcal{T}$ with a rotated square mesh having four triangular regions in the first column. Define

$$\mathcal{M}_{10} := \{\mu \in L^2(\mathcal{T}) \mid \mu = \sum_{n=1}^{10} \alpha_n \mu_n\}$$

where $\alpha_n \in \mathbb{R}$ and $\mu_1, \mu_2, \cdots, \mu_{10}$ are the characteristic functions of the regions defined by the triangles/diamonds (see Figure 3.6). Using the μ and $\mathcal{M}_{10}$ described above, we calculate both the projection $\hat{\mu}$ of μ onto $\mathcal{M}_{10}$ and $\bar{\mu}$ found by solving Problem 3.1.2. The L^∞ difference between $\hat{\mu}$ and $\bar{\mu}$ is less than 1×10^{-12}.

Next we approximate the Preisach measure μ in a space of continuous functions. Discretize $\mathcal{T}$ using a rotated square mesh grid with 17 nodes along the s-axis. Let

$$\mathcal{M}_{153} := \{\mu \in L^2(\mathcal{T}) \mid \mu = \sum_{n=1}^{153} \beta_n \mu_n\}$$

where $\beta_n \in \mathbb{R}$ and μ_n is the function created when $\mu_n = 1$ at the nth node, $\mu_n = 0$ at all other nodes (the standard tent function used in finite element approximation schemes). Again we calculate both the projection $\hat{\mu}$ of μ onto $\mathcal{M}_{153}$ and $\bar{\mu}$ found by solving Problem 3.1.2. In this case, however, the difference between the projection $\hat{\mu}$ of μ onto $\mathcal{M}_{153}$ and $\bar{\mu}$ is much greater. This is apparent when comparing Figure 3.7 with Figure 3.8. In this case, $\|\hat{\mu} - \bar{\mu}\|_\infty > 0.1$.

These results point out the error introduced when the Preisach state functions are not in the span of the basis vectors of $\mathcal{M}_N$. While, in some ways, it may seem advantageous to approximate the Preisach measure μ by a continuous function, this will invariably introduce errors because of the discontinuity inherent to the Preisach state functions.

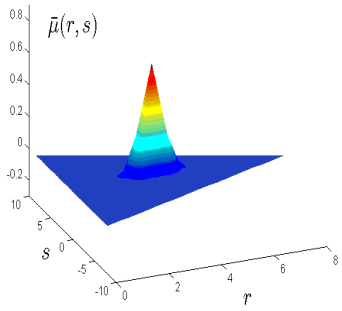

Figure 3.7: Graph of the projection $\hat{\mu}$ of μ onto $\mathcal{M}_{153}$.

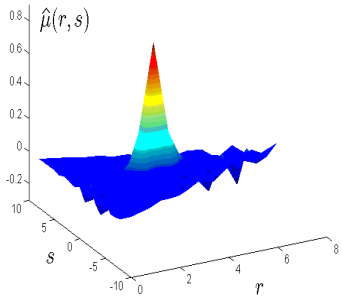

Figure 3.8: Graph of $\bar{\mu}$, the solution to Problem 3.1.2.

3.3 Approximations using experimental data

In the last section we used our approximation scheme with simulated data. In this section we will use the approximation scheme with experimental data taken from SMA wire to investigate the feasibility of the proposed identification method to identify a set of model parameters that result in an accurate hysteresis model.

The experimental setup shown in Figure 3.9 was used to generate identification and test data. The experimental setup consists of an 8 in. length of NiTi alloy wire suspended vertically with a 50 gram mass attached to the

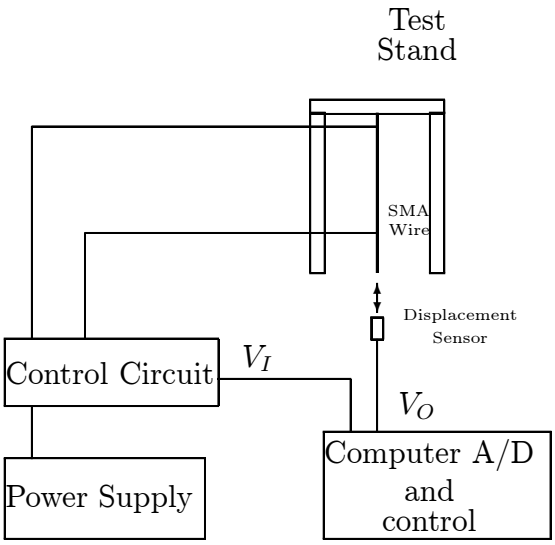

Figure 3.9: Experimental Setup

lower end. A displacement sensor is located at the lower end of the wire to measure the change in length of the wire. The length of the wire is controlled by heating the wire with a current. A two channel data acquisition system was used to record a voltage proportional to the input current and a voltage from the displacement sensor. For convenience these voltages will be referred to as the input V_I and output V_O voltages. Using this setup, data for use in identifying the model parameters, and data for testing the resulting Preisach model, were collected.

The data used for identification of the model parameters was obtained by varying the input voltage to produce a set of desired reversal curves. The sequence of input voltages was predetermined by the method described in Section 3.1.

A complete input cycle required to generate the desired reversal curves for identification consists of 11 subcycles. For each subcycle, the input voltage begins at zero and it is stepped up to a desired maximum and then stepped down to zero. The maximum of each subcycle is incremented for each successive cycle until the wire temperature exceeds the temperature at which it is fully in the austenite phase. At each step within each subcycle the input voltage is held constant for 60 seconds to allow the wire temperature to stabilize. Examples of the control input voltage and the output voltage are shown in

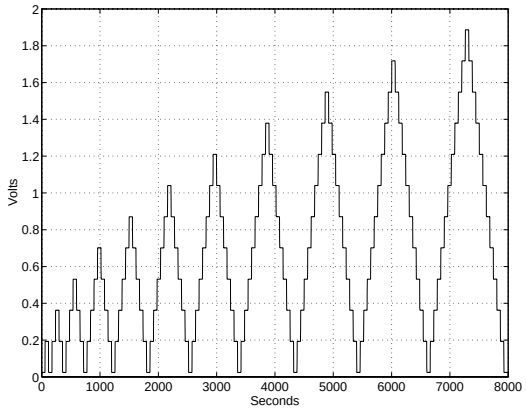

Figure 3.10: Step input voltage for identification.

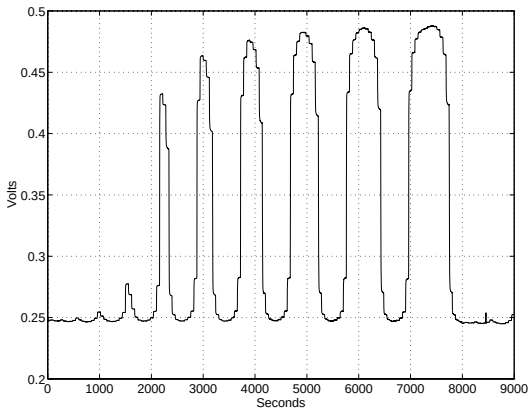

Figure 3.11: Output voltage for identification.

Figure 3.10 and Figure 3.11.

The input and output voltages were sampled at a 0.5 Hz rate during the entire run (typically 10,000 seconds). The I/O data used for the identification process is an average of the last 5 samples of data collected at each input level. A plot of an example of this averaged I/O data is given in Figure 3.12. The I/O hysteresis is obvious. Using this type of data, the model parameters were identified.

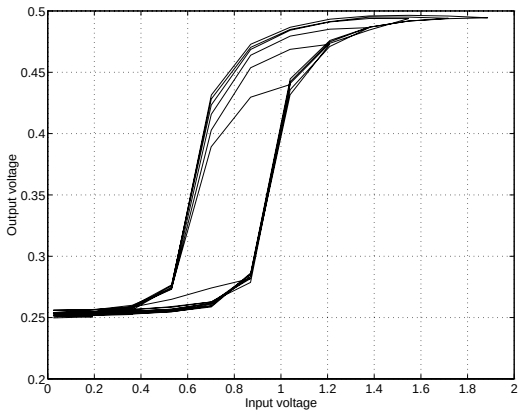

Figure 3.12: I/O hysteresis

Figure 3.13 shows the training data and our predictions of what the training data should be using the model parameters identified. Figure 3.14 shows a set of first order reversal curves emanating from the limiting descending branch and the predictions of those reversal curves using identified parameters.

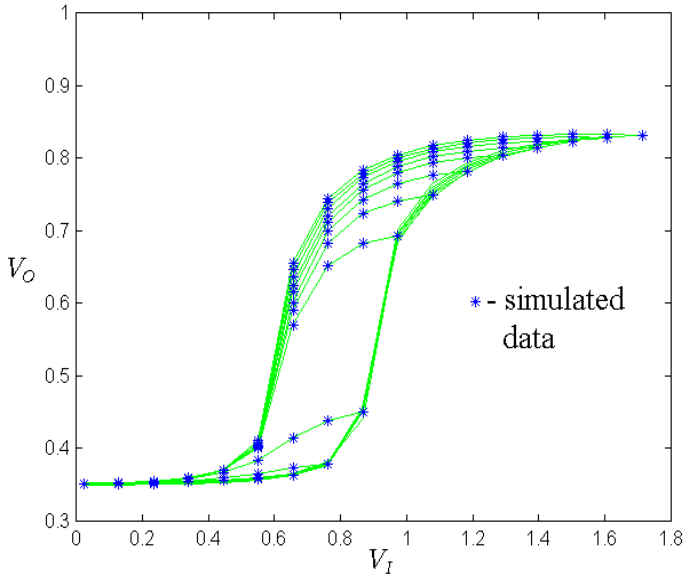

Figure 3.13: Experimental training data vs. approximations obtained from non-singular measures.

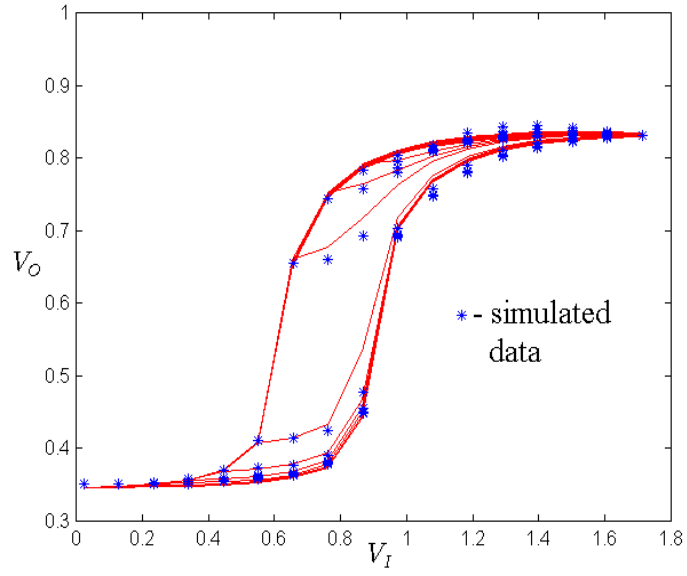

Figure 3.14: Experimental first order reversals vs. approximations obtained from non-singular measures.

Chapter 4

Extending the Method to Singular Measures

The Preisach measure is often viewed as a probability distribution on the Preisach plane, and hence it is assumed to be a non-negative, bounded function (certainly having no singularities). While this may be compelling from a physical standpoint, it introduces restrictions which may limit the models utility. As Mayergoyz discusses in [15] there is no need to make this assumption if we view the Preisach model as a phenomenological model.

An inherent property of Preisach operators with non-singular measures is that the initial slope of all reversal curves must be zero. In a number of physical systems, however, reversal curves with non-zero initial slope have been observed. In this chapter, we examine the problem of trying to approximate singular Preisach measures. We focus on singularities located on the boundary of the Preisach plane. A singular measure concentrated along the boundary of the Preisach plane yields reversal curves with non-zero initial slope. (Note that due to the congruency property all reversal curves from a point $u(t) = u_1$ will have the same slope). This type of singularity is by far the most common model used in practice.

There is some material in this chapter which is very similar to material in Chapter 3. This was done in order to present this chapter in a more self-contained manner.

4.1 Theoretical background for singular measures

Our first task is to choose an appropriate setting in which to study the singular Preisach measures. The goal, as before, is to take advantage of the duality relationship between the measure and the state of the Preisach plane while allowing for a somewhat general space of measures. We accomplish this by defining a new space of *singular Preisach measures*.

$$\mathbb{M} := \{\text{finite Borel measures } \mu \text{ on } \mathcal{P} \mid \mu = \mu^I(r,s) + k(s)\delta(r)\}$$

Here $\mu^I \in L^2(\mathcal{P})$, $k \in L^2(\mathbb{R})$, δ is the Dirac delta, and the support of μ is contained in $\mathcal{T}$. It is important to point out here that $\mu \in \mathbb{M}$ implies that μ satisfies (2.7), and thus by Theorem 2.1.2, μ yields a continuous Preisach operator. We now make the following definitions for μ, $\nu \in \mathbb{M}$:

$$\langle \mu, \nu \rangle_{\mathbb{M}} := \langle \mu^I, \nu^I \rangle_{L^2(\mathcal{T})} + \langle k^\mu, k^\nu \rangle_{L^2(-C,C)} = \int_{\mathcal{T}} \mu^I \nu^I \, ds \, dr + \int_{-C}^{C} k^\mu k^\nu \, ds$$

$$\|\mu\|_{\mathbb{M}} := \sqrt{\langle \mu, \mu \rangle_{\mathbb{M}}}$$

It is easy to see that under $\langle \cdot, \cdot \rangle_{\mathbb{M}}$, $\mathbb{M}$ is a Hilbert space.

We also define a new class of *Preisach state functions* $\mathbb{S}$ to be a class of measures on the Preisach plane of the form

$$\xi = \xi^I(r,s) + h(s)\delta(r)$$

where

- $B_\xi = \text{graph}(\phi)$ for some $\phi \in M$,
- $\xi^I : \mathcal{P} \to \{1, -1\}$, and
- $h(s) = \text{trace}(\xi^I)$ along $r = 0$.

If we restrict the support of the state functions to $\mathcal{T}$ then, $\mathbb{S} \subset \mathcal{M}$. Note that in our description of the evolution of the relays above, we have tacitly defined a *state operator*

$$C[0,t] \ni u(\cdot) \mapsto \xi_{u(t)} \in \mathbb{S}$$

that describes the evolution of the state functions with changes in the input function u.

Now, for a given $\mu \in \mathbb{M}$ we define the Preisach operator $\mathcal{H}_\mu : C[0,T] \to \mathbb{R}$ by

$$\mathcal{H}_\mu(u(t)) = \langle \xi_{u(t)}, \mu \rangle_{\mathbb{M}}.$$

Once again, we can think of the Preisach operator as the composition of the nonlinear *state operator*

$$C[0,t] \ni u(\cdot) \mapsto \xi_{u(t)} \in \mathbb{S}$$

with the linear inner product pairing between the state functions and a fixed Preisach measure

$$\mathbb{S} \ni \xi_{u(t)} \mapsto \langle \xi_{u(t)}, \mu \rangle_{\mathbb{M}} \in \mathbb{R}.$$

Likewise, we think of the inner product action

$$\langle \xi, \mu \rangle_{\mathbb{M}}$$

as an *observation* of the measure $\mu \in \mathbb{M}$ under the state $\xi \in \mathbb{S}$.

We again consider the problem of finding the optimal approximation of the Preisach measure $\mu \in \mathbb{M}$ in a finite dimensional subspace of $\mathbb{M}$.

Problem 4.1.1 (Identification from a given singular measure). Suppose $\mu \in \mathbb{M}$ is given and $\mathbb{M}_N$ is an N dimensional subspace of $\mathbb{M}$. Given a set of Preisach state functions $\{\xi_i\}_{i=1}^M$ and corresponding observations of the measure μ, $d_i = \langle \xi_i, \mu \rangle_{\mathbb{M}}$, find $\bar{\mu} \in \mathbb{M}_N$ such that

$$\sum_{i=1}^{M} |\langle \xi_i, \bar{\mu} \rangle_{\mathbb{M}} - d_i|^2 = \min_{\widetilde{\mu} \in \mathbb{M}_N} \sum_{i=1}^{M} |\langle \xi_i, \widetilde{\mu} \rangle_{\mathbb{M}} - d_i|^2 \tag{4.1}$$

$$= \min_{\widetilde{\mu} \in \mathbb{M}_N} \sum_{i=1}^{M} |\langle \xi_i, \widetilde{\mu} - \mu \rangle_{\mathbb{M}}|^2 \tag{4.2}$$

Ideally, the solution of this problem would give us the unique projection of μ onto the finite dimensional subspace $\mathbb{M}_N$. The projection is the solution of the following problem.

Problem 4.1.2 (Best approximation to a given singular measure). Given $\mu \in \mathbb{M}$ and an N-dimensional subspace $\mathbb{M}_N \subset \mathbb{M}$, find $\hat{\mu} \in \mathbb{M}_N$ that provides the "best approximation" to μ in $\mathbb{M}_N$, i.e.

$$\|\hat{\mu} - \mu\|_{\mathbb{M}} = \min_{\widetilde{\mu} \in \mathbb{M}_N} \|\widetilde{\mu} - \mu\|_{\mathbb{M}} \tag{4.3}$$

Theorem 3.1.1 ensures us that the solution to Problem 4.1.1 is the solution to Problem 4.1.2 if we prescribe a set of training data $\{\xi_i\}_{i=1}^{M}$ such that

$$\xi_i \in \mathbb{M}_N \text{ for } 1 \leq i \leq N. \tag{4.4}$$

$$A = \begin{bmatrix} a_{1,1} & a_{1,2} & \cdots & a_{1,N} \\ a_{2,1} & a_{2,2} & \cdots & a_{2,N} \\ \vdots & & \ddots & \vdots \\ a_{M,1} & a_{M,2} & \cdots & a_{M,N} \end{bmatrix} \text{ is full rank.} \tag{4.5}$$

(Here $a_{i,j} = \langle \xi_i, \mu_j \rangle_{\mathbb{M}}$ where $\mu_1, \mu_2, \cdots, \mu_N$ are the basis elements of $\mathbb{M}_N$).

Due to the inherent discontinuities in the Preisach state functions, we must approximate in a space of discontinuous functions if we want to satisfy Equation 4.4. We begin with a rotated square mesh discretization of the limiting triangle $\mathcal{T}$ in which the s-axis is divided into n even subintervals (Figure 4.1). Our first n basis elements $\mu_1, \mu_2, \cdots, \mu_n$ are singular measures: the characteristic functions of the intervals on the s-axis created by the mesh. The remaining $(n^2+n)/2$ basis elements $\mu_{n+1}, \mu_{n+2}, \cdots, \mu_N$ are the characteristic functions of the triangular and diamond shaped regions. (Here $N = \frac{n^2+3n}{2}$.) Our finite dimensional approximation space can now be represented as

$$\mathbb{M}_N := \{\mu \in \mathbb{M} \mid \mu = \sum_{i=1}^{N} \alpha_i \mu_i\}$$

where $\alpha_i \in \mathbb{R}$.

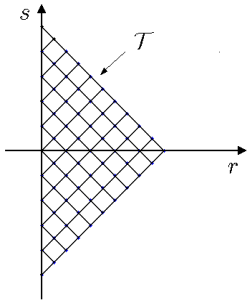

Figure 4.1: Rotated square mesh discretization of $\mathcal{T}$

Unfortunately it is impossible to simply extend the theory from Chapter 3 to this problem. There are N basis elements for $\mathbb{M}_N$ but only $N-n$ possible unique states ξ_i that satisfy Equation 4.4. In adding the singular measures, we increased the dimension of the space of possible measures, but not the number of possible state functions, since the singular part of the state function is constrained by the trace relation. Thus, we can not satisfy Equations 4.4 and 4.5 simultaneously. In general $\bar{\mu}$ (the solution to Problem 4.1.1) will not be equal to $\hat{\mu}$ (the unique projection of μ onto $\mathbb{M}_N$). What can we say about $\|\hat{\mu} - \bar{\mu}\|_{\mathbb{M}}$?

For any $\mu \in \mathbb{M}_N$ we can write

$$\mu = \hat{\mu} + \nu = \sum_{j=1}^{N} \langle \mu, \mu_j \rangle_{\mathbb{M}} + \nu = \sum_{j=1}^{N} \beta_j \mu_j + \nu$$

where $\nu \in \mathbb{M}_N^{\perp}$. Also for $\xi_i \in \mathbb{S}$ we can write

$$\xi_i = \sum_{j=1}^{N} a_{i,j} \mu_j + l_i$$

where $a_{i,j}$ is as in Equation 4.5 and $l_i \in \mathbb{M}_N^{\perp}$. Thus, for any $\widetilde{\mu} = \sum_{i=1}^{N} \alpha_i \mu_i \in \mathbb{M}_N$ we have

$$\begin{aligned}
\sum_{i=1}^{M} |\langle \xi_i, \widetilde{\mu} - \mu \rangle_{\mathbb{M}}|^2 &= \sum_{i=1}^{M} |\langle \sum_{j=1}^{N} a_{i,j}\mu_j + l_i, \sum_{k=1}^{N} (\alpha_k - \beta_k)\mu_k - \nu \rangle_{\mathbb{M}}|^2 \\
&= \sum_{i=1}^{M} |\sum_{j=1}^{N} a_{i,j} \sum_{k=1}^{N} (\alpha_k - \beta_k) \langle \mu_j, \mu_k \rangle_{\mathbb{M}} - \langle l_i, \nu \rangle_{\mathbb{M}}|^2 \\
&= \sum_{i=1}^{M} |\sum_{j=1}^{N} a_{i,j} (\alpha_j - \beta_j) - \langle l_i, \nu \rangle_{\mathbb{M}}|^2
\end{aligned}$$

Note that the error between $\hat{\mu}$ and $\bar{\mu}$ occurs only when $\langle l_i, \nu \rangle_{\mathbb{M}} \neq 0$, for if $\langle l_i, \nu \rangle_{\mathbb{M}} = 0$ for all i then

$$\bar{\mu} = \min_{\widetilde{\mu} \in \mathbb{M}_N} \sum_{i=1}^{M} |\langle \xi_i, \widetilde{\mu} - \mu \rangle_{\mathbb{M}}|^2 \quad \Longrightarrow \quad \alpha_j = \beta_j \quad \Longrightarrow \quad \bar{\mu} = \hat{\mu}$$

Although we have no control over ν, we can control l_i by our choice of ξ_i. We call $\{\mu_j \mid B_\xi \bigcap \text{interior}(\mu_j) \neq \emptyset\}$ the *remnant* of $\mathbb{M}_N$ under ξ. Clearly, support$\{l_i\} \subset$ remnant of $\mathbb{M}_N$ under ξ_i. It is reasonable then to make the remnant small in order to reduce $\|\hat{\mu} - \bar{\mu}\|_{\mathbb{M}}$. This can be accomplished by choosing $\{\xi_i\}_{i=1}^M$ in the following manner.

- We begin with the initial state of negative saturation. We then record state functions and data from first reversal curves with incrementally higher input extrema.
- The input extrema, and the data collection points (with the exception of the first data collection point after an input reversal) correspond to the boundaries between the n triangular regions along the s-axis in our discretization.
- The first data point after the reversal is recorded when the input is half way between the boundaries (see Figure 4.2, 4.3 and 4.4). Hence, these state functions are not contained in $\mathbb{M}_N$, but the remnant for each are limited to one triangular basis element and its adjacent singular basis element.

Before we investigate the solution to Problem 4.1.1 in the subspace $\mathbb{M}_N$ with the set of state functions $\{\xi_i\}_{i=1}^N$ prescribed above, let us look at a similar problem posed on a $(N-n)$-dimensional subspace that incorporates the boundary constraints that the state functions must satisfy. That is we will form a subspace $\mathbb{M}'_{N-n} \subset \mathbb{M}_N$ by combining each singular basis element of $\mathbb{M}_N$ with the triangular element adjacent to it. Thus our basis elements for $\mathbb{M}'_{N-n}$ are the following.

$$\begin{aligned}
\mu'_1 &= \mu_1 + \mu_{n+1} \\
\mu'_2 &= \mu_2 + \mu_{n+2} \\
&\vdots \\
\mu'_n &= \mu_n + \mu_{2n} \\
\mu'_{n+1} &= \mu_{2n+1} \\
&\vdots \\
\mu'_{N-n} &= \mu_N
\end{aligned}$$

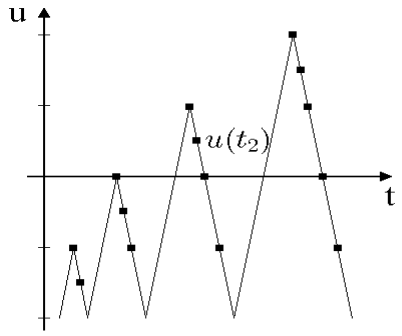

Figure 4.2: Sample input with data collection points for singular measure.

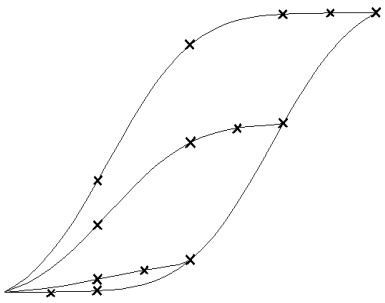

Figure 4.3: Hysteresis loop with data collection points for singular measures.

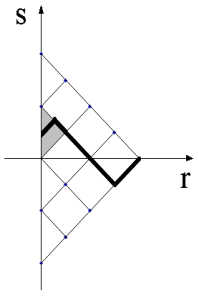

Figure 4.4: Graph of the memory curve $\phi_{u(t_2)}$ corresponding to $\xi_{u(t_2)}$. The remnant is shaded.

Problem 4.1.3. Given $\mu \in \mathbb{M}$, find $\mu' \in \mathbb{M}'_{N-n}$ such that

$$\begin{aligned}\sum_{i=1}^{M} |\langle \xi_i, \mu' \rangle_{\mathbb{M}} - d_i|^2 &= \min_{\widetilde{\mu} \in \mathbb{M}_N} \sum_{i=1}^{M} |\langle \xi_i, \widetilde{\mu} \rangle_{\mathbb{M}} - d_i|^2 \\ &= \min_{\widetilde{\mu} \in \mathbb{M}_N} \sum_{i=1}^{M} |\langle \xi_i, \widetilde{\mu} - \mu \rangle_{\mathbb{M}}|^2\end{aligned}$$

In this case, a set $\{\xi_i\}_{i=1}^{N-n}$ consisting of the state functions above with no remnant satisfies (4.4) and (4.5). This assures us that μ' is the projection of μ onto $\mathbb{M}'_{N-n}$. However, $\mu_{2n+1} = \mu'_{n+1}, \cdots, \mu_N = \mu'_{N-n}$. And since the bases for both spaces are orthogonal, the components of μ' corresponding to the basis elements represented by the diamond shaped regions in Figure 4.1 (we will call this region the *interior* of $\mathbb{M}_N$) are the same as the corresponding components of the projection of μ onto the larger space $\mathbb{M}_N$.

With this in mind, let us return to the problem of approximating $\mu \in \mathbb{M}$ in the subspace $\mathbb{M}_N$. Finding a solution to Problem 3.1.2 is equivalent to finding $\bar{x} \in \mathbb{R}^N$ such that $|A\bar{x} - d|^2 \leq |Ax - d|^2$ for all $x \in \mathbb{R}^N$. Arranged properly, A can be written in block form.

$$A\bar{x} - d = \begin{bmatrix} A_{1,1} & A_{1,2} & A_{1,3} \\ A_{2,1} & A_{2,2} & A_{2,3} \\ A_{3,1} & A_{3,2} & A_{3,3} \end{bmatrix} \begin{bmatrix} \bar{x}_1 \\ \bar{x}_2 \\ \bar{x}_3 \end{bmatrix} - \begin{bmatrix} d_1 \\ d_2 \\ d_3 \end{bmatrix} \tag{4.6}$$

where the first n rows of A, $\begin{bmatrix} A_{1,1} & A_{1,2} & A_{1,3} \end{bmatrix}$, result from the state functions with non-trivial remnant and the next n rows, $\begin{bmatrix} A_{2,1} & A_{2,2} & A_{2,3} \end{bmatrix}$, represent the state functions just prior to reversal. The first n columns of A, $\begin{bmatrix} A_{1,1} \\ A_{2,1} \\ A_{3,1} \end{bmatrix}$, represent the singular measure and the next n columns, $\begin{bmatrix} A_{1,2} \\ A_{2,2} \\ A_{3,2} \end{bmatrix}$, represent the adjacent triangular regions. $\bar{x}_1 \in \mathbb{R}^n$ contains the coefficients for the singular elements, $\bar{x}_2 \in \mathbb{R}^n$ contains the coefficients for the triangular elements and $\bar{x}_3 \in \mathbb{R}^{N-2n}$ contains the coefficients for the diamond shaped regions.

From the structure of the matrix A we have

$$A_{2,1} = A_{2,2} \tag{4.7}$$

$$A_{3,1} = A_{3,2} \tag{4.8}$$

By substituting Equations (4.7) and (4.8) into Equation (4.6) we get

$$A\bar{x} - d = \begin{bmatrix} A_{1,1} & A_{1,2} & A_{1,3} \\ A_{2,2} & A_{2,2} & A_{2,3} \\ A_{3,2} & A_{3,2} & A_{3,3} \end{bmatrix} \begin{bmatrix} \bar{x}_1 \\ \bar{x}_2 \\ \bar{x}_3 \end{bmatrix} - \begin{bmatrix} d_1 \\ d_2 \\ d_3 \end{bmatrix} \tag{4.9}$$

The last two block-rows of this system can be written as

$$\begin{bmatrix} A_{2,2} & A_{2,3} \\ A_{3,2} & A_{3,3} \end{bmatrix} \begin{bmatrix} \bar{x}_1 + \bar{x}_2 \\ \bar{x}_3 \end{bmatrix} = \begin{bmatrix} d_2 \\ d_3 \end{bmatrix} \tag{4.10}$$

This is, in essence, Problem 4.1.3. The coefficients in $\bar{x}_3$ give us the projection of μ onto the interior of $\mathbb{M}_N$. The following theorem sums up our findings.

Theorem 4.1.1. *Given a set of Preisach state functions $\{\xi_i\}_{i=1}^N \in \mathbb{S}$ chosen according to the method outlined above, the identification problem for any measure $\mu \in \mathbb{M}$ yields the projection of μ onto the interior of $\mathbb{M}_N$.*

In other words we have "localized" the error between $\hat{\mu}$ and $\bar{\mu}$ to the singular elements and their adjacent triangular elements.

$$\begin{aligned} \|\hat{\mu} - \bar{\mu}\|_{\mathbb{M}} &= \|\sum_{i=1}^{N} \beta_i \mu - \sum_{j=1}^{N} \alpha_i \mu\|_{\mathbb{M}} \\ &= \|\sum_{i=1}^{2n} (\beta_i - \alpha_i)\mu\|_{\mathbb{M}} + \|\sum_{i=2n+1}^{N} (\beta_i - \alpha_i)\mu\|_{\mathbb{M}} \\ &= \|\sum_{i=1}^{2n} (\beta_i - \alpha_i)\mu\|_{\mathbb{M}} \end{aligned}$$

4.2 Approximations using simulated data

In this section we will demonstrate the ability of least squares to determine the projection of a given measure $\mu \in \mathbb{M}$ on the interior of $\mathbb{M}_N$ by solving Problem 4.1.1. For our simulation we will combine a form of the Preisach measure given by Della Torre [10, p.41] with a singular measure along the boundary of the Preisach plane. Specifically, we will use

$$\mu(r, s) := \mu^I(r, s) + k(s)\delta(r)$$

where

$$\mu^I(r,s) = \frac{2}{\pi}\exp[-2((r-3.5)^2+s^2)]$$

$$k(s) = 0.05\exp[-2(s-3.5)^2] + 0.1\exp[-2(s+3.5)^2]$$

(see Figure 4.5 and Figure 4.6)

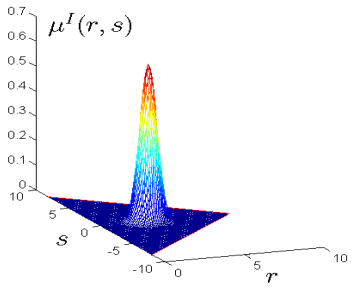

Figure 4.5: Graph of $\mu^I(r,s)$, the nonsingular part of μ.

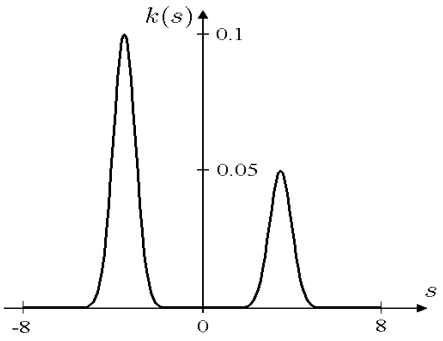

Figure 4.6: Graph of $k(s)$, the singular part of μ.

We will approximate μ in the space

$$\mathbb{M}_{14} := \{\mu \in \mathcal{M} \mid \mu = \sum_{n=1}^{14} \alpha_n \mu_n\}$$

(see Figure 4.7)

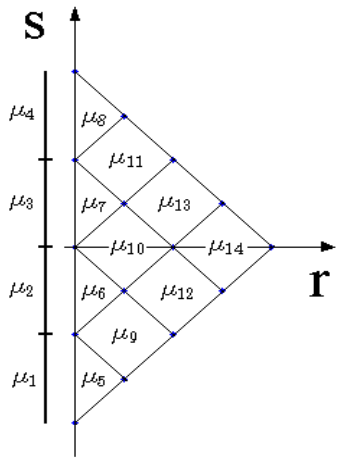

Figure 4.7: Regions of $\mathcal{T}$ in $\mathbb{M}_{14}$.

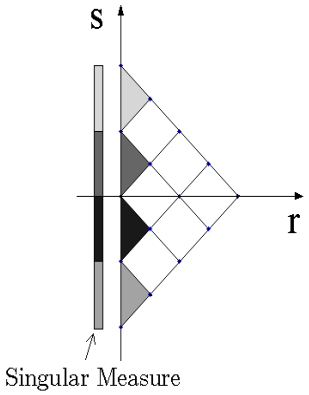

Figure 4.8: The difference in $\bar{\mu}$ and $\hat{\mu}$ on $\mathbb{M}_{14}$.

where $\alpha_i \in \mathbb{R}$, $\mu_1, \mu_2, \mu_3, \mu_4$ are the characteristic functions of the intervals on the s-axis created by a rotated square mesh discretization of the limiting triangle $\mathcal{T}$, $\mu_5, \mu_6, \mu_7, \mu_8$ are the characteristic functions of the triangular regions, and $\mu_9, \cdots, \mu_{14}$ are the characteristic functions of the diamond shaped regions respectively.

We calculate $\bar{\mu} = \sum_{i=1}^{14} \alpha_i \mu_i = \sum_{i=1}^{14} \bar{\mu}_i$, the solution to Problem 4.1.1, and $\hat{\mu} = \sum_{j=1}^{14} \beta_j \mu_j = \sum_{j=1}^{14} \hat{\mu}_i$, the projection of μ onto $\mathbb{M}_N$. Now we see that $\|\hat{\mu}_i - \bar{\mu}_i\|_\infty = \mid \beta_i - \alpha_i \mid < 1 \times 10^{-12}$ for $9 \leq i \leq 14$. The solution to Problem 4.1.1 has given us the projection of μ onto the interior of $\mathbb{M}_N$. However, $.005 \leq \|\hat{\mu}_i - \bar{\mu}_i\|_\infty = \mid \beta_i - \alpha_i \mid \leq .05$ for $1 \leq i \leq 8$. The solution to Problem 4.1.1 has not given us the projection of μ onto the singular measure or the triangular regions adjacent to the boundary of the Preisach plane. This is illustrated in Figure 4.8. The darker regions indicate a greater L^∞ error.

4.3 Approximations using experimental data

In this section we use experimental data from SMA wire to demonstrate the utility of our approximation scheme. The experimental setup is identical to that in Section 3.3. In this experiment, however, we will use the data collection points suggested by the method in Section 4.1. Figure 4.9 shows the training data and the predictions of the training data using the singular measure approximation scheme.

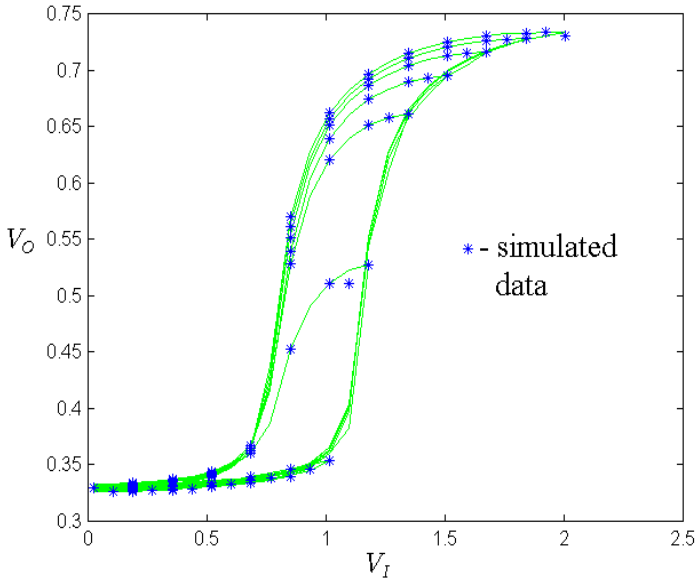

Figure 4.9: Experimental data vs. approximated data obtained from singular measures.

Chapter 5

Conclusions

The duality between the state of the Preisach plane and Preisach measure μ leads to an excellent setting in which to study the Preisach operator. The focus of this work was to take advantage of this duality while approximating the parameter μ in the somewhat general setting L^2. This allows us to approximate μ using least squares, a desirable method in terms of adaptive parameter identification.

The use of least squares can introduce errors into the approximation unless appropriate choices of the approximation space and training data are made. Although the physics of a system may suggest that approximation in a continuous space is desirable, it has been shown here that this will almost certainly introduce errors because of the inherent discontinuities in the state operators.

Theorem 3.1.1 assures us that with the proper choices of approximation space and training data, least squares will yield the projection of a given Preisach measure in $L^2(\mathcal{T})$ onto the approximation space. Clearly this is a theoretical result which can not be achieved in an experimental setting. The ability of the model to absorb experimental error becomes critical when trying to apply this method. In the method described, this ability rests upon the conditioning of the matrix A. This matrix is highly structured and has a relatively small condition number. Thus experimental error will not be greatly amplified in the approximation of μ.

While we are not able to determine the projection of a singular measure onto an approximation space, we can restrict the error of the approximation to the singular elements and the triangular regions adjacent to the singular elements. Nothing can currently be said, however, about the error in the remnant elements. For this reason, and because data collection is a discrete process, it is recommended that the measure μ be approximated in a space of non-singular measures even if singularities are expected.

We have treated this method in the setting of the scalar Preisach model. Extensions of this method to various modifications of the Preisach model, including the moving model and vector models, should be possible and are the focus of further research.

Bibliography

[1] Attard, Phil. "Interaction and deformation of elastic bodies: origin of adhesion hysteresis," *Journal of Physical Chemistry. B,* 104:10635.

[2] Banks, H.T., A. Kurdila, and G. Webb, 1996. "Identification of hysteretic control influence operators representing smart actuators. Part I: formulation," CRSC-TR96-14.

[3] Beattie, C, J. Rossi, and R.C. Rogers. 2001. *Notes on Matrix Theory* http://www.math.vt.edu/people/beattie/5524/MtrxThryBk/.

[4] Bertotti, G. 1998. *Hysteresis in Magnetism,* Academic Press, San Diego.

[5] Brokate, M. and J. Sprekels. 1996. *Hysteresis and Phase Transitions,* Springer-Verlag, Berlin.

[6] Brown, W.F. Jr.. 1962. *Magnetostatic Principles in Ferromagnetism,* North-Holland Publishing Company, Amsterdam.

[7] Contreras, Samuel M., Timothy R.H. Davies. 2000. "Course-grained debris-flows: hysteresis and time-dependent rheology," *Journal of Hydraulic Engineering,* 126:938.

[8] Darity, William Jr., Arthur H. Goldsmith. 1996. "Unemployment, Social Psychology and Unemployment Hysteresis," *Journal of Post Keynesian Economics.* 16:55-71.

[9] Della Torre, E. and F. Vajda. 1994. "Parameter identification of the complete-moving-hysteresis model using major loop data," *IEEE Transactions on Magnetics,* 30:4987-5000.

[10] Della Torre, E. 1999. *Magnetic Hysteresis,* IEEE Press, New Jersey.

[11] Hock, H.S., J.A.S. Kelso, G. Schoner. 1993, "Bistability, hysteresis, and phase transitions in the perceptual organization of apparent motion," *Journal of Experimental Psychology: Human Perception and Performance.* 19:63-80.

[12] Hughes, D., J.T. Wen. 1994. "Preisach modeling and compensation for smart material hysteresis," *SPIE Active Materials and Smart Structures,* 2427:50-63.

[13] Inabi, M., M. Fujikawa, Z. Ogumi. 2000. "Calorimetric study of the hysteresis in the charge-discharge profiles of mesocarbon microbeds heat-treated at low temperatures," *Journal of the Electrochemical society.* 147:4008.

[14] Krasnoselskii, M.A., A.V. Pokrovskii. 1989. *Systems with Hysteresis,* Springer Verlag, Berlin.

[15] Mayergoyz, I.D. 1991. *Mathematical Models of Hysteresis,* Springer, New York.

[16] Oti, John, Edward Della Torre. 1990. "A vector moving model of both reversible and irreversible magnetizing processes," *Journal of Applied Physics.* 67:5364-5366.

[17] Oti, J., F. Vajda, and E. Della Torre. 1991. "Identification of parameters in a moving model," *Journal of Applied Physics* 69:4826-4828.

[18] Parreira, C., C. Enachescu, F. Varret. 2000. "A two-sublattice model for light-induced hysteresis in spin-crossover solids: symmetry breaking and kinetic effects," *Journal of Physics. Condensed Matter* 12:9395.

[19] Polak, J., F. Fardoun, S. Degallaix. 2001. "Analysis of the hysteresis loop in stainless steels I. Austenitic and ferritic steels," *Materials Science & Engineering. A, Structural Materials,* 297:144.

[20] Preisach, F. 1935."Über die magnetische nachwirkung," *Z. Phys.,* 94:277-302.

[21] Sazykina, T.G., V.V. Alekseev, A.I. Kryshev. 2000. "The self-organization of trophic structure in ecosystem models: the succession phenomena, trigger regimes and hysteresis," *Ecological Modeling.* 133:83.

[22] Stoner, E.C., E.P. Wohlfarth. 1948. "A mechanism of magnetic hysteresis in heterogeneous alloys," *Philos. Trans. Royal Soc. London.* 240:599-642.

[23] Visintin, A. 1994. *Differential Models of Hysteresis,* Springer-Verlag, Berlin.

[24] Weeds, Helen. 1999. "'Reverse hysteresis': R& D investment with stochastic innovation," *The Warwick Economics Research Paper Series.* #578.

[25] Xia, Guoshou, Joseph J. Pignatello. 2001. "Detailed sorption isotherms of polar and apolar compounds in a high-organic soil," *Environmental Science & Technology.* 35:84.

[26] Xu, C., Z.Y. Li, P.M. Hui. 2001. "Monte Carlo studies of hysteresis curves in magnetic composites with fine magnetic particles," *Journal of Applied Physics* 89:3403.

Vita

Daniel S. Joseph

Education:

2001 PhD in Mathematics
Virginia Tech, Blacksburg, VA

1999 MS in Mathematics
Virginia Tech, Blacksburg, VA

1991 BS in Mathematics
Virginia Military Institute, Lexington, VA

Work Experience:

1997-2001 Virginia Tech, Blacksburg, VA
Mathematics Department, Graduate Teaching Assistant

1995-1997 U.S. Navy, SWOS, Newport, RI
Gas-Turbine Engineering Instructor

1991-1995 U.S. Navy, USS Moosbrugger DD-980
Division Officer

Publications:

"Parameter identification for Preisach models of hysteresis," in preparation.

"Parameter identification for Preisach operators with singular measures," in preparation.